Desalination and Water Treatment
www.deswater.com

doi: 10.1080/19443994.2015.1112308

57 (2016) 20671–20682
September

Taylor & Francis
Taylor & Francis Group

Optimization of magnetic-seeding coagulation in artificially polluted surface water treatment by response surface methodology

Zhaoyang Su, Xing Li*, Yanling Yang, Meiling Xu, Yixuan Ding, Zhiwei Zhou

College of Architecture and Civil Engineering, Beijing University of Technology, No. 100, Xi Da Wang Road, Chao Yang District, Beijing 100124, P.R. China, Tel. +86 10 67391726; emails: SZY_BJUT@163.com (Z. Su), lixing@bjut.edu.cn (X. Li), yangyanling@bjut.edu.cn (Y. Yang), xmlyuxin1104@163.com (M. Xu), dyxbjut@163.com (Y. Ding), hbzzwbjut@163.com (Z. Zhou)

Received 17 March 2015; Accepted 18 October 2015

ABSTRACT

Artificially polluted surface water was treated using magnetic-seeding coagulation, with polyaluminum chloride (PAC) as the coagulant and a ferromagnetic material as the magnetic seed (MS). A novel approach using a combination of response surface methodology (RSM) and the Box–Behnken design (BBD) was employed to evaluate the effects and interactions of four main factors, the dosages and dosing points of PAC and MS. The three response variables selected to evaluate the effectiveness of the treatment were supernatant turbidity removal rate, floc size, and floc strength. The optimal operating conditions were obtained by constraining the three desirable responses using Minitab software. The PAC and MS dosages (22.7 mg/L and 0.6 g/L) and their dosing points (1.5 and 1.2 min) were determined to be the optimum conditions for the maximum turbidity removal rate, floc size, and floc strength of 98.0%, 154.7 μm, and 57.8%, respectively. Confirmation experiments demonstrated that such a combination of RSM and BBD was a powerful and effective approach for optimizing the magnetic-seeding coagulation. Additionally, zeta potential analysis indicated that the MS decreases the negative charge of pollutants and acts as a coagulating core during coagulation.

Keywords: Magnetic-seeding coagulation; Floc size; Floc strength; Flocculation index; Response surface methodology

1. Introduction

In water and wastewater treatment, the coagulation/flocculation process is an essential process by which various colloidal or suspended particles are aggregated into large flocs and are then removed using separation processes, such as sedimentation, flotation, and filtration [1–4]. Two commonly used methods used for enhancing coagulation performance are as follows: (1) increasing the coagulant dosage, and (2) adjusting the pH of the untreated water [5]. Magnetic-seeding coagulation, which combines magnetic materials and coagulants, is one way to optimize the coagulation process. It has been tested for effectiveness and has certain advantages, such as larger handling capacity, better effluent quality, and comparatively lower energy consumption [6,7]. Hence, magnetic-seeding coagulation is a prospective technique that is of great interest to many researchers.

*Corresponding author.

Magnetic separation is a step that usually follows magnetic-seeding coagulation. The seeding of ferromagnetic materials, which enables magnetic field makes magnetic collection and separation possible, and broadens the scope of traditional magnetic separation, which can only remove nonmagnetic pollutants. During this separation, the seeded flocs can be rapidly and efficiently attracted and then eliminated using magnets. This is because the strong magnetic force (F_m) acts on seeded flocs when they are exposed to a magnetic field (H):

$$F_m = V\, M(H)\, \mathrm{d}H/\mathrm{d}x \quad (1)$$

where V is the volume of the seeded floc, $M(H)$ is the magnetization of the seeded floc, and $\mathrm{d}H/\mathrm{d}x$ is the magnetic field gradient.

As indicated in Eq. (1), we find that the value of F_m is directly proportional to the volume of floc. Theoretically, the larger the size of the seeded floc, the larger is the F_m. Thus, pollutants can be easily captured on a filter matrix by making use of the magnetic tractive force (F_m), which overcomes other competing forces such as gravitation, hydrodynamics and inertia. In an open gradient system, the magnetic tractive force combined with gravitation can accelerate the precipitation process of the flocs.

Previous studies have demonstrated that when flocs are subjected to a high shear force, the residual turbidity increases because of floc breakage [8–10]. In addition, Li et al. noted that the filtration rate of magnetic separation can reach up to five times that of conventional quartz sand filtration [11]. Thus, magnetic seeded flocs need to be much stronger to resist a large shear force. Therefore, floc strength is a significant operational parameter in this particular solid/liquid separation method. However, as indicated in Eq. (1), there is a contradiction between increasing floc size and greater strength. Recent research has focused primarily on the performance of magnetic-seeding coagulation [12–15], and little attention has been paid to the significance of the constrained relationship between the strength and size of seeded flocs, which partially limits the application of the magnetic separation technique.

This study is the first attempt to systematically study the optimization of the constrained condition between the size and the strength of the seeded flocs, in an effort to enhance subsequent magnetic separation. Therefore, the overall purpose of this research is to model and optimize the magnetic seeding process using response surface methodology (RSM), where PAC and magnetic seed (MS) dosages and their dosing points are chosen as experimental variables. The three response variables are residual turbidity, floc strength, and floc size. The results attempt to achieve the optimal constrained magnetic-seeding conditions that will improve the removal efficiency of the non-magnetic contaminants using magnetic separation.

2. Materials and methods

2.1. Raw water and magnetic seed

All the reagents used were analytical grade. PAC (with 28% Al_2O_3 content, basicity of 72.3%, from FuChen, Tianjin, China), used as coagulant, was dissolved into Milli-Q deionized water to obtain a 50 g/L stock solution. Kaolin clay (Imerys, St. Austell, Cornwall, UK) was used as a natural colloid stock suspension (128 g/L) prepared according to Ref. [8]. Humic acid, sodium salt (HA, Aldrich, Cat: H1, 675-2), was dissolved to form a stock solution of concentration 5 g/L, and the preparation was similar to that reported by Yu et al. [16].

Both kaolin clay and humic acid stock solutions were used to simulate polluted surface water, stabilized at room temperature for 24 h before the experiment with the local (Beijing, China) tap water. The main physicochemical characteristics of the untreated water were as follows: turbidity 40.2 NTU, zeta potential −15.7 mV, temperature 17.5℃ and pH 7.6.

The seeding material used in this study was provided by BLINK Water Purifying Agent Factory and its characteristics were obtained for a specific surface area of 8.712 m^2/g and an average size of 60 μm. The material consisted of ferromagnetic iron oxide, as well as weak magnetic substances, such as calcium oxide and silica, which could be magnetically coagulated and trapped. It was washed after the supernatant was clear and then dried in the oven at a temperature of 105℃ for at least 5 h before storage.

2.2. Magnetic-seeding coagulation trials

A series of jar tests were performed in a six-paddle stirrer with impellers equipped with 50 mm (L) × 40 mm (W) rectangular blades (ZR4-6, Zhongrun Water Industry Technology Development Co., Ltd, China) to determine the optimum dosages of PAC and MS, as well as their dosage ranges. Seeding tests were carried out at the optimum PAC dosage of 26 mg/L (calculated as PAC) and constant initial pH of about 7.3. The jar tests for seeding coagulation were initially begun with rapid mixing at 350 rpm ($G = 449\ s^{-1}$). After 0.5 min, a predetermined dosage of PAC was added with or without MS (0.2, 0.4, and 0.6 mg/L,

respectively), with 1.5 min of rapid mixing at 350 rpm (dosing points 0.5, 1.0, and 1.5 min, calculated from the start of initial mixing); then the blender was subsequently adjusted to a slow mixing at 50 rpm ($G = 33\ s^{-1}$) for 12 min followed by a 3-min settling period. Finally, the supernatant was collected from the sample port for the measurement of residual turbidity.

2.3. RSM experimental design

RSM is an empirical mathematical and statistical modeling technique for multiple regression analysis, based on properly designed experiments to solve multivariable equations, and simultaneously evaluates the relative significance of several factors even in the presence of complex interaction [17].

Experimental data were analyzed using the statistical analysis system under the Box–Behnken design (BBD) and fitted to a specific polynomial model. The quadratic equation for the variables was as follows:

$$Y = \beta_0 + \sum_{i=1}^{j} \beta_i X_i + \sum_{i=1}^{k} \beta_{ii} X_i^2 + \sum_{i}^{i<j} \sum_{j} \beta_{ij} X_i X_j \quad (2)$$

Y is the predicted response, β_0 a constant; β_i the first-order model coefficient; β_{ii} the squared coefficient for the factor i, and β_{ij} the linear model coefficient for the interaction between factors i and j. The Design Expert Software (version 8.0.5, Stat-Ease, Inc., Minneapolis, MN) was used for the statistical design of experiments and for data analysis.

Model terms were selected or rejected based on the P value (probability) with a 95% confidence level. To assess the "goodness of fit" of this model, the results obtained were then analyzed using analysis of variance (ANOVA) using the Fisher's statistical method. As reported, the determination coefficient (R^2) gives the proportion of the total variation in the response predicted by the model, suggesting the ratio of the sum of squares due to regression (SSR) to total sum of squares (SST). A high R^2 value, close to 1, is desirable and a reasonable agreement with R^2_{Adj} is necessary [18]. In addition, adequate precision (AP) compares the range of the predicted values at the design points to the average prediction error. This ratio greater than 4 illustrates adequate model discrimination [17]. The coefficient of variance (CV) as the ratio of the standard error of estimate to the mean value of the observed response defines reproducibility of the model. A model can normally be considered reproducible if its CV value is not greater than 10% [19].

Three-dimensional (3D) plots and their corresponding contour plots were obtained based on the effects of the four factors at three levels. Furthermore, the optimum region was identified based on the main parameters in the overlaid plot. The adequacy of the regression equations was checked by comparing the experimental data with predicted values obtained from the equations.

2.4. Floc size analysis

During the slow mixing period, flocs samples were obtained from below the surface of the suspension using a hollow glass tube with an inner diameter of 5 mm. The tube with both ends open was inserted 2.5 cm below the surface. Then one end was covered by a finger and the sample was withdrawn carefully and transferred onto a flat microscope slide. The images of flocs in this sample were captured using an optical microscope (Olympus, BX51TF, Japan) with a CCD camera. The camera has a sensor matrix consisting of 1,280 (horizontal) × 1,024 (vertical) pixels. To interpret the image sizes correctly, a graduated microscale was photographed to determine the number of pixels corresponding to a given standard length. Images were obtained from an interrogation window of about 2,230 × 1,784 pixels and a resolution of 574 pixels/mm was achieved. Thus, 1 pixel corresponds to about 1.7 μm. All images were recorded on the hard drive of a PC and processed using Image pro software to obtain the mean values of floc size. In this study, Feret diameter was measured and the floc size was determined as an arithmetic mean based on at least 80 samples.

2.5. Measurement of floc strength

Experiments on the kinetics of the formation and breakage of seeded flocs were conducted using the Photometric Dispersion Analyzer (PDA-2000, Rank Brothers, UK) based on the "turbidity fluctuation" technique. The experimental procedure was similar to that of Yukselen and Gregory [9]. The mixing procedures were as follows: a rapid mixing at 350 rpm ($G = 449\ s^{-1}$) for 0.5 min, then 1.5 min of rapid mixing at 350 rpm ($G = 449\ s^{-1}$) followed by a slow mixing period of 12 min at 50 rpm ($G = 33\ s^{-1}$). Finally, the flocs were exposed to an increased shear of 350 rpm ($G = 449\ s^{-1}$) for 1 min to investigate their strength.

The average transmitted light intensity (dc value) through the flowing sample and the root-mean-square value (rms) of the fluctuating component were monitored. The ratio (rms/dc) indicates a sensitive

measurement of particle aggregation and is defined as an indicator called flocculation index (FI) [20]. In this study, the FI was recorded by a PC data acquisition system at 2 s intervals after reaching an initial steady value.

Flocs strength factor (S_f) is a well-established parameter for describing floc strength during the flocs breakage phase, and can be calculated as shown in Eq. (3), according to Ref. [21]. V_1 is the maximum FI value before the flocs breakage, and V_2 is the FI value when the flocs are broken after intensive stirring.

$$S_f = V_2/V_1 \times 100 \quad (3)$$

Here, S_f indicates the resistance of the formed flocs to the increasing shear force. The larger the S_f is, the less sensitive to breakage the floc is, which is therefore considered as the stronger.

2.6. Zeta potential analysis

The variation of zeta potential during the process of coagulation was measured using the Zetasizer Nano2000 (Malvern Instruments Ltd, UK). The measurements were carried out after PAC and/or MS addition during the 1.5-min rapid mixing period.

3. Results and discussion

The results of the preliminary jar test (control group) indicated that the optimum dosage of PAC was 24 mg/L with 84.49% turbidity removal rate, 107.9 μm floc size, and 38.3% floc strength. Under the optimum dosage of PAC, the dosage of MS was determined to be 0.4 g/L with the turbidity removal rate reaching up to 96.35%. Hence, 10–30 mg/L and 0.2–0.6 g/L were chosen as the dosage ranges of PAC and MS, respectively, from the technical and economic perspective.

3.1. Experimental results of RSM

The response variables, including turbidity removal rate, floc strength, and floc size, were obtained from 29 groups of experiments including parallel control groups and were summarized in Table 1. Each experiment was conducted three times and the mean value was used during analysis.

3.1.1. Data analysis of turbidity removal rate as the response variable

The equations derived using ANOVA were modified by eliminating the statistically insignificant terms. The following equation represents the empirical relationship in the form of a modified polynomial between the turbidity removal rate (Y_1) and the other four factors ($X_1 - X_4$).

$$\begin{aligned} Y_1 = {} & 120.24 - 0.45X_1 - 51.86X_2 - 6.42X_3 - 20.44X_4 \\ & + 1.69X_1X_2 + 0.46X_1X_3 + 0.07X_1X_4 - 4.08X_2X_3 \\ & + 29.88X_2X_4 - 0.02X_1^2 + 23.33X_2^2 + 27.93X_3^2 \\ & + 1.17X_4^2 + 0.02X_1^2X_3 - 0.69X_1X_2^2 - 1.73X_1X_3^2 \\ & - 13.16X_2^2X_4 \end{aligned} \quad (4)$$

The result of ANOVA for the turbidity removal rate, shown in Table 2, indicates that the equation fitted well and the *F*-statistic was insignificant, implying a significant model correlation between the variables and the process responses.

Specifically, the critical values of this model with significant coefficients were as follows: $R^2 = 0.9816$, $R^2_{Adj} = 0.9531$, $R^2_{Pred} = 0.7868$, CV = 0.4%, AP = 22.214. Consequently, values for the simplified model ensured a satisfactory adjustment of the model to the experimental data.

The significance testing for the coefficient of the equation was conducted and the related variables are listed in Table 3. Values of "Prob. > *F*" less than 0.05 indicate that the model terms are significant. In linear terms, PAC dosage and its dosing point and MS dosage were significant and unique, and played decisive roles in the flocculating process. Conversely, the dosing point of MS was not significant since it's "Prob. > *F*" value was 0.8978, which is greater than 0.05. Therefore, the higher order effects, such as the quadratic terms for PAC and MS dosage, were significant. The interaction terms with significant effects are shown in Fig. 1(a)–(c), respectively.

Fig. 1(a) shows the change in turbidity removal rates with the dosage and dosing point of PAC varying within the experimental ranges, while those of MS are kept constant at a central level. The shape of the curve and the curvature of the contour at the bottom indicate that both factors have a quadratic effect on the turbidity removal rate in composite process. It is observed that at a low level of PAC dosage, the corresponding dosing point has no apparent effect on it. However, in comparison, a high PAC dosage level (~30 mg/L) causes the target response value to increase sharply when the dosing point varies from 0.5 to 1.5 min, ultimately reaching its peak value. This target obviously becomes easier to reach when the concentration of PAC is kept at central level. This phenomenon suggests that a variation over time could produce a limiting effect on the target value for a

Table 1
BBD design and response values

	Real values				Response		
Run	X_1 (mg/L)	X_2 (min)	X_3 (g/L)	X_4 (min)	Y_1 (%)	Y_2 (μm)	Y_3 (%)
1	10	0.5	0.4	1	94.3	103.5	58.7
2	30	0.5	0.4	1	90.9	123.9	60.6
3	10	1.5	0.4	1	94.5	103.4	55.9
4	30	1.5	0.4	1	97.3	164.6	46.7
5	20	1	0.2	0.5	95.7	120.8	47.4
6	20	1	0.6	0.5	96.7	139.8	60.8
7	20	1	0.2	1.5	95.4	112.9	47.7
8	20	1	0.6	1.5	96.7	136.6	60.0
9	10	1	0.4	0.5	94.4	109.7	58.7
10	30	1	0.4	0.5	96.8	144.9	52.0
11	10	1	0.4	1.5	94.0	117.8	56.1
12	30	1	0.4	1.5	97.8	137.6	53.2
13	20	0.5	0.2	1	92.7	100.1	51.3
14	20	1.5	0.2	1	96.1	125.3	44.5
15	20	0.5	0.6	1	95.1	127.4	64.2
16	20	1.5	0.6	1	96.9	143.7	62.7
17	10	1	0.2	1	93.3	106.6	45.5
18	30	1	0.2	1	94.7	116.9	48.6
19	10	1	0.6	1	95.4	125.2	59.7
20	30	1	0.6	1	97.4	165.0	54.7
21	20	0.5	0.4	0.5	96.9	125.3	55.9
22	20	1.5	0.4	0.5	98.0	142.8	53.7
23	20	0.5	0.4	1.5	91.8	113.8	57.8
24	20	1.5	0.4	1.5	96.5	135.9	57.6
25	20	1	0.4	1	96.9	137.4	53.4
26	20	1	0.4	1	96.4	132.0	54.1
27	20	1	0.4	1	95.9	134.2	53.0
28	20	1	0.4	1	96.2	136.1	55.0
29	20	1	0.4	1	96.0	142.3	55.2

Notes: X_1: PAC dosage, X_2: PAC dosing point, X_3: magnetic seed dosage, X_4: magnetic seed dosing point; Y_1: turbidity removal rate, Y_2: floc size, Y_3: floc strength.

Table 2
ANOVA for turbidity removal rate

Item	Sum of squares	Degrees of freedom	Mean square	*F*-value	Prob. > *F*
Model	84.16	17	4.95	34.48	<0.0001
Residual	1.58	11	0.14	–	–
Lack of fit	0.95	7	0.14	0.86	0.5947
Pure error	0.63	4	0.16	–	–

Notes: R^2: determination coefficient, R^2_{Adj}: adjusted R^2, R^2_{Pred}: predetermined R^2, CV: coefficient of variation, AP: adequate precision. Values for the reduced model with significant coefficients, $R^2 = 0.9816$, $R^2_{Adj} = 0.9531$, $R^2_{Pred} = 0.7868$, CV = 0.4%, AP = 22.214.

proper dosage of 20 mg/L or more. Further, it could also be concluded that an unnecessarily long period of rapid mixing may be not good for turbidity removal as it causes the formations of the seeded flocs to weaken.

Fig. 1(b) shows that, when the dosing points of PAC and MS are at central level, the turbidity removal rate can reach an anticipated value at a high quantity of MS when the dosage of PAC is approximately 30 mg/L, indicating that a higher dosage of MS is a

Table 3
Significance of quadratic model coefficient of turbidity removal rate

Independent variables	Regression coefficients freedom	Degrees of freedom	Standard error	Prob. > F
X_1	1.56	1	0.19	<0.0001
X_2	1.47	1	0.11	<0.0001
X_3	0.67	1	0.13	0.0004
X_4	0.018	1	0.13	0.8978
X_1X_2	1.56	1	0.19	<0.0001
X_1X_3	0.15	1	0.19	0.4495
X_1X_4	0.35	1	0.19	0.0914
X_2X_3	−0.41	1	0.19	0.0544
X_2X_4	0.89	1	0.19	0.0006
X_1^2	−0.94	1	0.15	<0.0001
X_2^2	−0.9	1	0.15	<0.0001
X_3^2	−0.27	1	0.15	0.101
X_4^2	0.29	1	0.15	0.074

more favorable condition for strengthening the seeding process. Further, excessive levels of PAC had a negative effect on the elimination of pollutants at a relatively low level MS dosage of 0.2 g/L, which agrees with the previous study using only PAC.

Fig. 1(c) indicates the importance of both dosing points on flocculating performance when the other two factors are kept at a central level. It can be seen that the target value will reach the peak gradually when the lag between two dosing points grows to 1 min. The maximum target value was obtained when the dosing points of PAC and MS were determined to be 1.5 and 0.5 min, respectively. This allowed MS to become the coagulating core and enabled hydrolyzed PAC to wrap it easily. Researchers have generally focused on the positive performance of the seeding coagulation activity of magnetic material [7,12]. However, this study demonstrated another effect, which is significant for settlement and dehydration processes, from the aspect of the dosing point.

3.1.2. Data analysis of floc size as the response variable

Eq. (5) represents the empirical relationship between the floc size (Y_2) and the other four factors ($X_1 - X_4$) in the form of a quadratic polynomial.

$$Y_2 = 73.04 - 0.12X_1 + 25.80X_2 + 79.76X_3 - 4.78X_4 + 2.04X_1X_2 + 3.69X_1X_3 - 0.05X_1^2 - 23.15X_2^2 - 111.08X_3^2 \quad (5)$$

The result of ANOVA for floc size, shown in Table 4, indicates that the second-order equation fitted well. Specifically model values of "Prob. > F" <0.0001 are less than 0.05 and the total determination coefficient R^2 is 0.9315. In terms of the difference in the value between R^2_{Adj} (0.899) and R^2_{Pred} (0.771), 0.128 < 0.2, and CV of 4.12% < 10%, both verified that the model constructed was of a high level of confidence and accuracy, while the AP value of 19.35 (>4) ensured that there was enough of the desired signal to offset the negative effects of unexpected noise.

The significance testing for the coefficients is indicated in Eq. (5), wherein the variables are expressed in terms of actual values listed in Table 5. In linear terms, the dosing point of the magnetic seed was the only insignificant factor which was the same as the result of the coefficient of Eq. (4) as mentioned in Section 3.1.1, while the " Prob. > F" values of other three factors were all below 0.0001, indicating the significance. However, to make a hierarchical control, this insignificant factor must be introduced in the model despite its seemingly contradictory attributes. In quadratic terms, PAC was highlighted significant and unique for the reason that excessive dosage of PAC led to the stabilization of the colloid suspension which could disaggregate the flocs again. The interaction terms with significant effects are depicted in Fig. 2(a) and (b), respectively.

Fig. 2(a) shows that the floc size is enhanced with the increase in the dosage and dosing point of PAC, while keeping those of MS are controlled at the central level, and it is also observed that the target value does not improve when either one of them is at a low level. Thus, we can deduce that a relatively high dosage of PAC at ~1.5 min contributes to the seeding performance, which is illustrated by using the floc size as an indicator. This phenomenon was in accordance with the previous analysis ($Y_1 \propto$ interaction between X_1 and X_2).

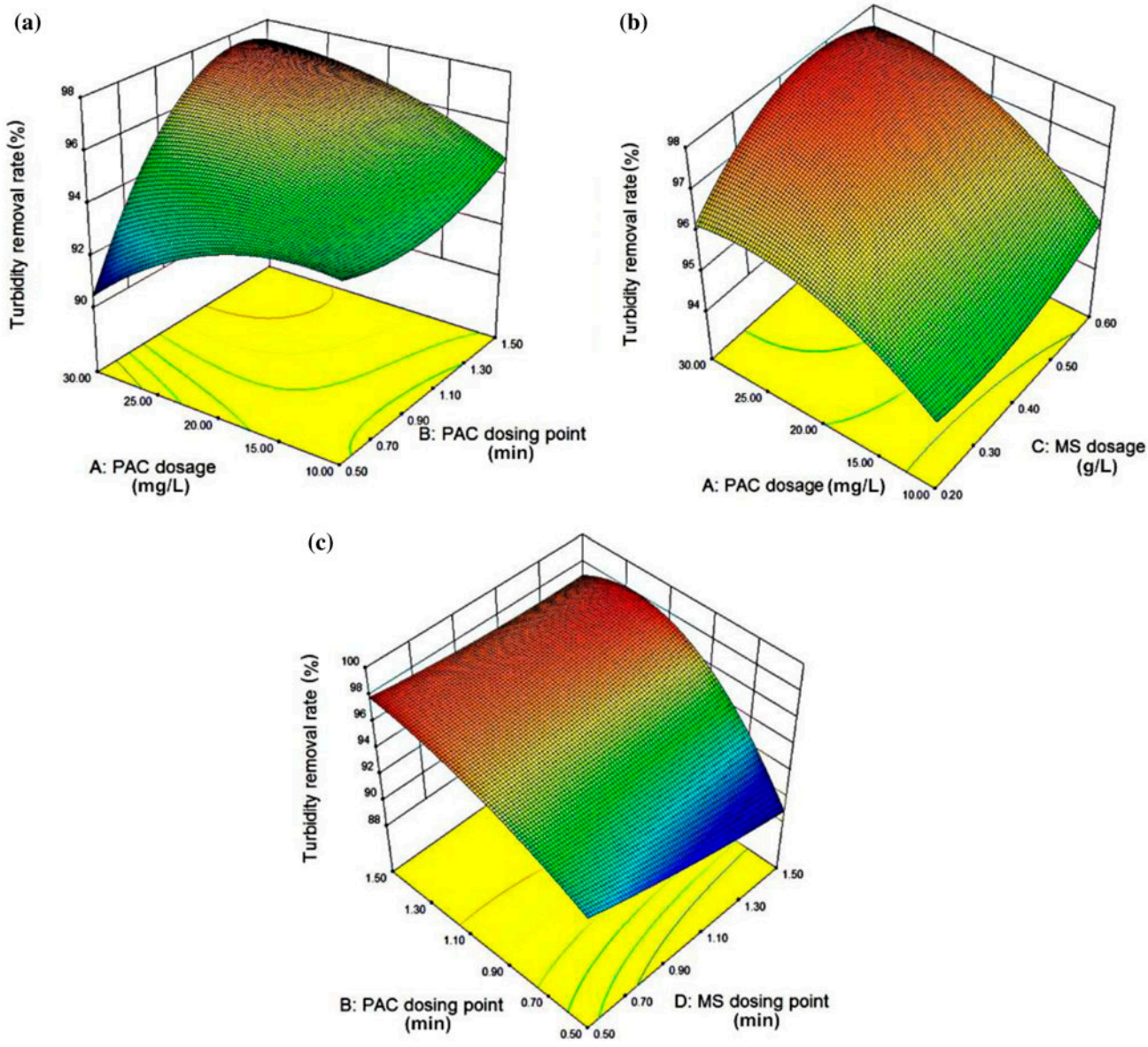

Fig. 1. 3D-Surface graphs of turbidity removal rate showing the interaction of variables ((a) PAC dosage–PAC dosing point, (b) PAC dosage–MS dosage, and (c) PAC dosing point–MS dosing point).

Table 4
ANOVA for floc size

Item	Sum of squares	Degrees of freedom	Mean square	*F*-value	Prob. > *F*
Model	7,230.84	9	803.43	28.7	<0.0001
Residual	531.87	19	27.99	–	–
Lack of fit	471.2	15	31.41	2.07	0.2519
Pure error	60.66	4	15.17	–	–

Notes: Values for the reduced model with significant coefficients, $R^2 = 0.9315$, $R^2_{Adj} = 0.899$, $R^2_{Pred} = 0.771$, CV = 4.12%, AP = 19.35.

Table 5
Significance of quadratic model coefficient of floc size

Independent variables	Regression coefficients freedom	Degrees of freedom	Standard error	Prob. > F
X_1	15.55	1	1.53	<0.0001
X_2	10.15	1	1.53	<0.0001
X_3	12.93	1	1.53	<0.0001
X_4	−2.39	1	1.53	0.1339
X_1X_2	10.2	1	2.65	0.0011
X_1X_3	7.37	1	2.65	0.0117
X_1^2	−4.61	1	2.04	0.0359
X_2^2	−5.79	1	2.04	0.0105
X_3^2	−4.44	1	2.04	0.0422

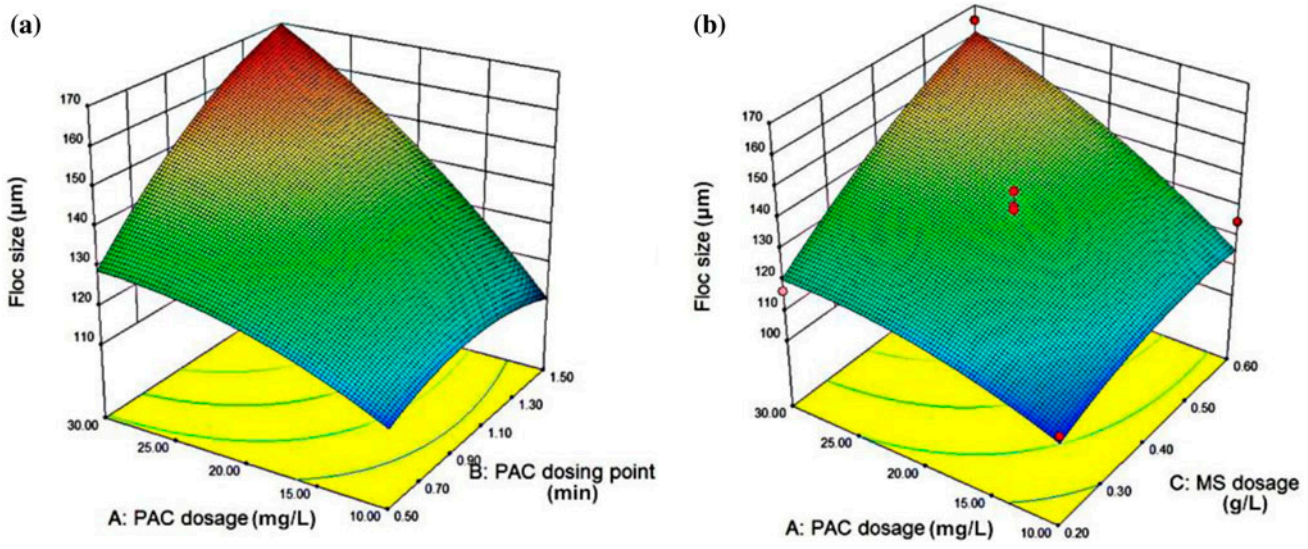

Fig. 2. 3D-Surface graphs of floc size showing the interaction of variables ((a) PAC dosage–PAC dosing point and (b) PAC dosage–MS dosage).

Fig. 2(b) displays an analogous tendency compared with Fig. 2(a), showing that the target response value will not vary significantly with a change in either variable when the other is kept at a low level. As Zhou et al. have observed, additives, including recycling sludge, microsand, magnetic seed and the like, can improve coagulation performance by acting as coagulating cores, which are then trapped by hydrolyzed coagulant [22]. Boller and Blaser [23] maintained that larger flocs generally settle down more quickly than smaller flocs of similar density. Hence, to form large flocs is one of the goals during sedimentation process, particularly following the magnetic-seeding coagulation process according to Eq. (1). Generally, larger flocs are also easier to break. However, few researchers have proposed a solution to this phenomenon during filtration, especially in magnetic separation at high filtration speeds (large G value) as mentioned in Section 1. Therefore, an analysis was conducted in the following section to reach a constrained optimum condition between the maximum values of floc size and floc strength.

3.1.3. Data analysis of floc strength as the response variable

Several studies have noted that floc strength, an important parameter, reflects the internal structure and the chemical bonds of formed aggregates to some extent. Jarvis et al. [24] pointed out that smaller flocs tend to have greater strength than larger flocs, while the use of magnetic seeding methods are aimed at

Table 6
ANOVA for floc strength

Item	Sum of squares	Degrees of freedom	Mean square	*F*-value	Prob. > *F*
Model	671.83	8	83.98	20.16	<0.0001
Residual	83.31	20	4.17	–	–
Lack of fit	79.83	16	4.99	5.73	0.0517
Pure error error	3.48	4	0.87	–	–

Notes: Values for the reduced model with significant coefficients, $R^2 = 0.8897$, $R^2_{Adj} = 0.8456$, $R^2_{Pred} = 0.6855$, CV = 3.73%, AP = 15.361.

Table 7
Significance of quadratic model coefficient of floc strength

Independent variables	Regression coefficients freedom	Degrees of freedom	Standard error	Prob. > *F*
X_1	−1.58	1	0.59	0.0143
X_2	−2.28	1	0.59	0.0009
X_3	6.43	1	0.59	<0.0001
X_4	0.31	1	0.59	0.6064
X_1X_2	−2.76	1	1.02	0.0135
X_1X_3	−2.04	1	1.02	0.0593
X_2^2	1.86	1	0.78	0.0266
X_3^2	−0.98	1	0.78	0.2212

attaining a larger floc size with a better magnetization function and/or an improved settlement performance.

Eq. (6) displays the empirical relationship between the floc strength (Y_3) and the other four factors ($X_1 - X_4$) in the form of a quadratic polynomial.

$$Y_3 = 32.82 + 0.80X_1 - 8.38X_2 + 72.18X_3 + 0.62X_4 - 0.55X_1X_2 - 1.02X_1X_3 + 7.44X_2^2 - 24.53X_3^2 \quad (6)$$

Table 6 summarizes the results of the analysis including the coefficients and ANOVA of the model. The analysis constructed a statistically significant model for the floc strength. Specifically, the values of R^2, R^2_{Adj}, R^2_{Pred}, CV, and AP were 0.8897, 0.8456, 0.6855, 3.73%, and 15.361, respectively, which were well fitted to the model according to the literature [17,18].

Table 7 illustrates the significance of each coefficient in the reduced quadratic model. In linear terms, magnetic dosing point was the only insignificant factor, while the other three factors were all proven to be significant, and this result was in accordance with the two previous response analyses. As indicated in Table 7, the dosage of MS was clearly the most decisive factor influencing floc strength. In quadratic terms, the significance of interaction was as follows: $X_1X_2 > X_2^2 > X_1X_3 > X_3^2$, as the "Prob. > *F*" values for them were 0.0135, 0.0266, 0.0593 and 0.2212 respectively.

Fig. 3(a) shows the interaction between PAC dosage and its dosing point and indicates that the target value reaches the maximum value when both factors are kept at relatively low level. However, this result is contrary to the optimized area of variables in the analyses of Y_1 and Y_2. Further, the dosage of PAC had no apparent influence on the target value, which was inconsistent with the findings [25], and may be caused by the special seeding process used.

Fig. 3(b) shows that magnetic seed dosage has a significant effect on floc strength regardless of PAC levels. The maximized target value was obtained when the dosage of MS was about 0.6 g/L and PAC dosage was 10 mg/L. The actual value of floc strength ranged from 44.49 to 64.23%, which was much higher than the 38.3% value for the control group. Hence, this model suggests that the seeding process contributed to the enhancement of flocs, which may be primarily caused by the chemical and physical bonds and merits further investigation.

3.2. Optimal coagulation condition

The main purpose of this section is to optimize a constrained condition that aims to ensure that each response value is maintained at the desired level. For multiple responses, the optimum condition where all parameters simultaneously meet the desirable criteria can visually be observed by superimposing or

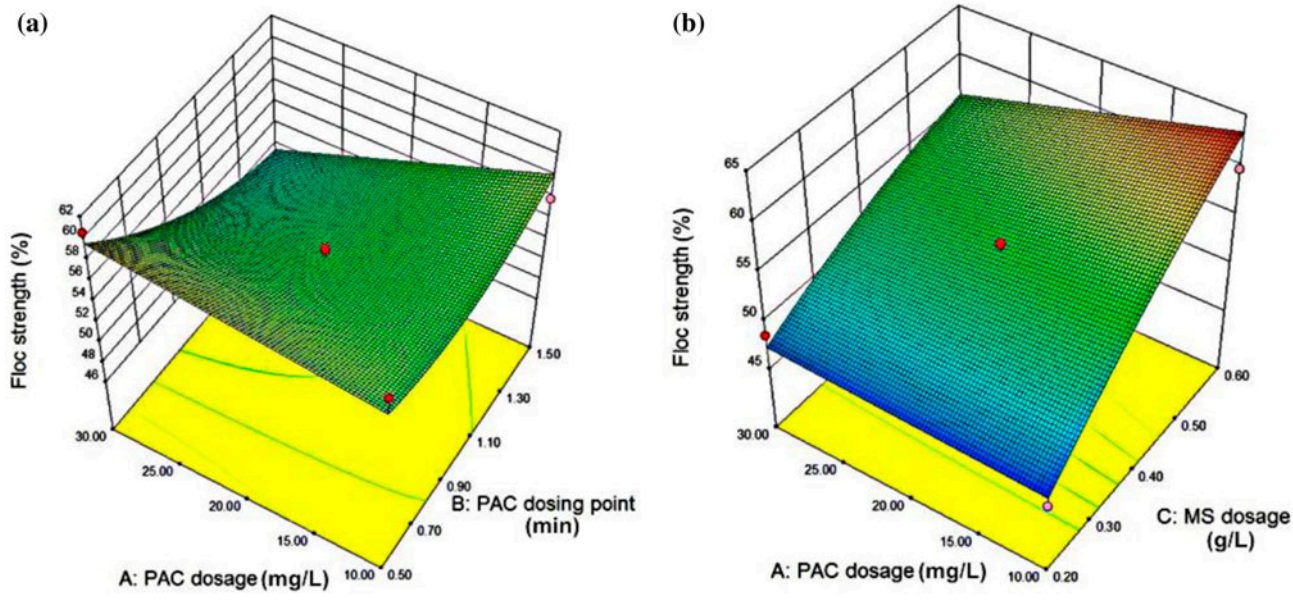

Fig. 3. 3D-Surface graphs of floc strength showing the interaction of variables ((a) PAC dosage-PAC dosing point and (b) PAC dosage-MS dosage).

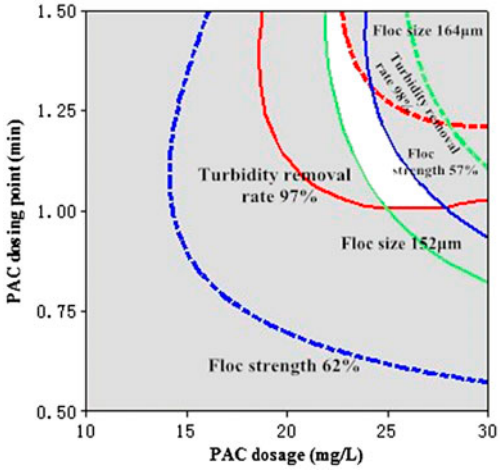

Fig. 4. Overlay plot for optimal region.

overlaying individual response contour on a contour plot. In this study, the interaction between X_1 and X_2 was significant, and was therefore, determined to be the critical response in optimization, as indicated in Tables 3, 5, and 7.

Fig. 4 depicts the optimum region, which is investigated based on the three critical responses ($Y_1 - Y_3$). The overlaid contour plot displays the area of feasible response values. The regions that fit the optimization criteria are whitened. The optimal condition for the magnetic seeding process was estimated using Minitab (version 15.0) to be: PAC dosage of 22.7 mg/L, PAC dosing point of 1.5 min, MS dosage of 0.6 g/L, and MS dosing point of 1.2 min. Meanwhile, the corresponding condition for water recovery efficiency was as follows: 98.0% turbidity removal rate, 154.7 μm floc size, and 57.8% floc strength. In addition, typical photographs of flocs under the control group and the optimized MS seeding condition can be observed in Fig. 5.

To confirm the validity of the statistical experimental strategy, an additional confirmation experiment with the optimal condition was conducted under identical conditions. Experimental findings for all response parameters were observed to be in close agreement with the model prediction. Specifically, the experimental results for ($Y_1 - Y_3$) were as follows: 97.2%, 156.4 μm and 58.7%, with low standard deviations of ±1.36%, ±0.89 μm, and ±2.33% respectively. This demonstrates that the RSM approach was appropriate for optimizing the operating conditions of the magnetic-seeding coagulation process.

3.3. Zeta potential analysis

The results of the zeta potential test during the process of magnetic seeding coagulation are shown in Fig. 6. The letters on the *x*-axis represent the different conditions of colloids/flocs for sampling, and the bars reveal the variation of zeta potential. Condition A shows that the zeta potential of untreated water was −15.73 mV without any additives. When compared to

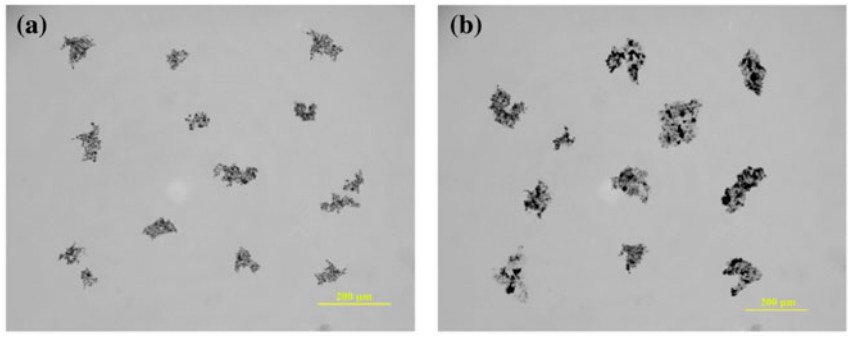

Fig. 5. Typical photographs of flocs ((a) the optimal PAC dosage of control group and (b) the optimized MS seeding condition).

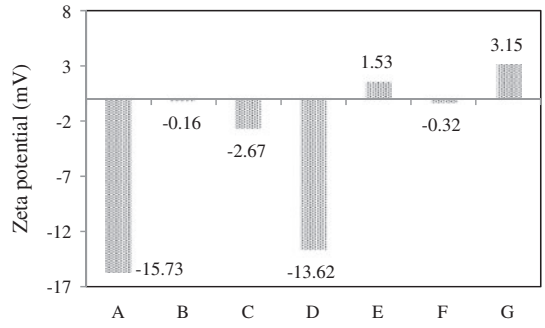

Fig. 6. Contrast of zeta potential in different condition ((A) untreated water without additives, (B) under the optimal PAC dosage of 24 mg/L of control group, (C) under the optimized PAC dosage of 22.7 mg/L of RSM, (D) under the dose of 0.6 g/L of magnetic seed, (E) magnetic seeding (0.6 g/L MS) condition B, (F) magnetic seeding (0.6 g/L MS) condition C, and (G) 0.6 g/L of magnetic seed in deionized water).

the bars for conditions B and C, it is clear that PAC has the strongest ability to modify the zeta potential of colloids and this result is attributed to the higher positive charge of PAC [26]. Additionally, condition B has been validated by Pefferkorm who has reported that the zeta potential should have a high correlation with the coagulant dosage if charge neutralization is the only process for coagulation, and that optimal removal efficiency will be attained when the zeta potential of the flocs is close to zero [27]. Simultaneously, the magnetic seeding process, as confirmed by conditions E and F, is bound to decrease negative charge by integrating with negative particles. Furthermore, condition G illustrates the positive charge of MS + 3.15 mV. Therefore, it can be deduced that MS decreases the negative charge of pollutants and acts as a coagulating core during seeding coagulation.

4. Conclusion

In this study, a novel approach, RSM, was employed to optimize operating conditions for the magnetic seeding coagulation process and to evaluate the effects of four main factors, the dosages and dosing points of PAC and MS, on the coagulation performance of flocs in terms of the supernatant turbidity, the floc size and the floc strength. An optimized condition of PAC dosage 22.7 mg/L, PAC dosing point 1.5 min, MS dosage 0.6 g/L and MS dosing point 1.2 min was obtained based on the three constrained desirable responses. Further investigation confirmed that RSM is an effective and powerful method to optimize the magnetic seeding coagulation process.

Acknowledgement

This research is funded by the National Natural Science Foundation of China (Grant No. 51478010).

References

[1] B.Q. Zhao, D.S. Wang, T. Li, C.W.K. Chow, C. Huang, Influence of floc structure on coagulation–microfiltration performance: Effect of Al speciation characteristics of PACls, Sep. Purif. Technol. 72 (2010) 22–27.
[2] M.Q. Yan, D.S. Wang, J.H. Qu, J.R. Ni, C.W.K. Chow, Enhanced coagulation for high alkalinity and micro-polluted water: The third way through coagulant optimization, Water Res. 42 (2008) 2278–2286.
[3] J.C. Wei, B.Y. Gao, Q.Y. Yue, Y. Wang, L. Lu, Performance and mechanism of polyferric-quaternary ammonium salt composite flocculants in treating high organic matter and high alkalinity surface water, J. Hazard. Mater. 165 (2009) 789–795.
[4] A. Zouboulis, G. Traskas, P. Samaras, Comparison of single and dual media filtration in a full-scale drinking water treatment plant, Desalination 213 (2007) 3 34–342.

[5] C. Volk, K. Bell, E. Ibrahim, D. Verges, G. Amy, M. LeChevallier, Impact of enhanced and optimized coagulation on removal of organic matter and its biodegradable fraction in drinking water, Water Res. 34 (2000) 3247–3257.
[6] R.D. Ambashta, M. Sillanpää, Water purification using magnetic assistance: A review, J. Hazard. Mater. 180 (2010) 38–49.
[7] M. Zhang, F. Xiao, X.Z. Xu, D.S. Wang, Novel ferromagnetic nanoparticle composited PACls and their coagulation characteristics, Water Res. 46 (2012) 127–135.
[8] W.Z. Yu, J. Gregory, L.C. Campos, Breakage and regrowth of flocs formed by charge neutralization using alum and polyDADMAC, Water Res. 44 (2010) 3959–3965.
[9] M.A. Yukselen, J. Gregory, The effect of rapid mixing on the break-up and re-formation of flocs, J. Chem. Technol. Biotechnol. 79 (2004) 782–788.
[10] M.A. Yukselen, J. Gregory, The reversibility of floc breakage, Int. J. Miner. Process. 73 (2004) 251–259.
[11] S.Q. Li, M.F. Wang, Z.A. Zhu, Q. Wang, X. Zhang, H.Q. Song, D.Q. Cang, Application of superconducting HGMS technology on turbid wastewater treatment from converter, Sep. Purif. Technol. 84 (2012) 56–62.
[12] Y.R. Li, J. Wang, Y. Zhao, Z.K. Luan, Research on magnetic seeding flocculation for arsenic removal by superconducting magnetic separation, Sep. Purif. Technol. 73 (2010) 264–270.
[13] T.J. Wan, S.M. Shen, S.H. Siao, C.F. Huang, C.Y. Cheng, Using magnetic seeds to improve the aggregation and precipitation of nanoparticles from backside grinding wastewater, Water Res. 45 (2011) 6301–6307.
[14] A. Merino-Martos, J. de Vicente, L. Cruz-Pizarro, I. de Vicente, Setting up high gradient magnetic separation for combating eutrophication of inland waters, J. Hazard. Mater. 186 (2011) 2068–2074.
[15] Y. Zhao, B.D. Xi, Y.R. Li, M.F. Wang, Z. Zhu, X.F. Xia, L.Y. Zhang, L.J. Wang, Z.K. Luan, Removal of phosphate from wastewater by using open gradient superconducting magnetic separation as pretreatment for high gradient superconducting magnetic separation, Sep. Purif. Technol. 86 (2012) 255–261.
[16] W.Z. Yu, J. Gregory, L. Campos, The effect of additional coagulant on the re-growth of alum-kaolin flocs, Sep. Purif. Technol. 74 (2010) 305–309.
[17] X.H. Xu, M.Z. He, Design of Experiment and Application of Design-Expert and SPSS, Science Press, Beijing, 2010.
[18] M.Y. Noordin, V.C. Venkatesh, S. Sharif, S. Elting, A. Abdullah, Application of response surface methodology in describing the performance of coated carbide tools when turning AISI 1045 steel, J. Mater. Process. Technol. 145(1045) (2004) 46–58.
[19] Q.K. Beg, V. Sahai, R. Gupta, Statistical media optimization and alkaline protease production from *Bacillus mojavensis* in a bioreactor, Process Biochem. 39 (2003) 203–209.
[20] R. Brothers, Photometric Dispersion Analyzer THE PDA 2000 Operating Manual, Cambridge, UK.
[21] C.S. Fitzpatrick, E. Fradin, J. Gregory, Temperature effects on flocculation, using different coagulants, Water Sci. Technol. 50 (2004) 171–175.
[22] Z.W. Zhou, Y.L. Yang, X. Li, W. Gao, H. Liang, G.B. Li, Coagulation efficiency and flocs characteristics of recycling sludge during treatment of low temperature and micro-polluted water, J. Environ. Sci. 24 (2012) 1014–1020.
[23] M. Boller, S. Blaser, Particles under stress, Water Sci. Technol. 37 (1998) 9–29.
[24] P. Jarvis, B. Jefferson, J. Gregory, S.A. Parsons, A review of floc strength and breakage, Water Res. 39 (2005) 3121–3137.
[25] W.Z. Yu, G.B. Li, Y.P. Xu, X. Yang, Breakage and regrowth of flocs formed by alum and PACl, Powder Technol. 189 (2009) 439–443.
[26] B.Y. Gao, Y.B. Chu, Q.Y. Yue, B.J. Wang, S.G. Wang, Characterization and coagulation of a polyaluminum chloride (PAC) coagulant with high Al_{13} content, J. Environ. Manage. 76 (2005) 143–147.
[27] E. Pefferkorn, Clay and oxide destabilization induced by mixed alum/macromolecular flocculation aids, Adv. Colloid Interface Sci. 120 (2006) 33–45.